The 17th Spacecraft Charging Technology Conference, Palais des Papes, Avignon, France, June 17-21, 2024

Development and Use of Spacecraft Charging Flight Constraints

Joseph I. Minow[1], Linda Neergaard Parker[2], Robert Meloy[3], Yihua Zheng[4], and Janessa Buhler[5]

[1]NASA Marshall Space Flight Center, Huntsville, Alabama, USA
[2]Space Weather Solutions, Huntsville, Alabama, USA
[3]SSAI, Goddard Space Flight Center, Greenbelt, Maryland, USA
[4]NASA Goddard Space Flight Center, Greenbelt, Maryland, USA
[5]NASA Kennedy Space Center, Florida, USA

***Abstract*—** Flight constraints in the form of launch commit criteria where launch operations are delayed if the criteria exceed a prescribed condition are often used to protect launch vehicles from extreme space environments during launch operations. Typically, these constraints are based on real-time measurements of the solar proton flux with a goal of avoiding single event upsets in mission critical avionics. Space environment flight constraints can also be used to avoid impacts from other space environments including meteor showers and spacecraft charging. This paper describes the development and use of spacecraft charging launch constraints that were used to protect the James Webb Space Telescope (JWST) from electrostatic discharge during the radiation belt transit following launch. We first introduce the use of space environment flight constraints and provide examples of where they have been used in the past. Then we describe the space weather launch commit criteria for solar particle events, internal charging, and surface charging adopted by JWST Program to protect the spacecraft from severe space environments during initial operations in the first 18 hours following launch. Finally, we summarize the space environment conditions present during the JWST launch operations when space weather turned out to not be a constraint for launch.

***Index Terms*—Spacecraft charging, On-Orbit Investigations, Flight Constraints**

I. INTRODUCTION

SPACECRAFT charging can interfere with launch vehicle and spacecraft operations through electrostatic discharge (ESD) damage of mission critical materials and avionics, phantom commands from arc generated radiofrequency noise coupling into sensitive electronics, and interference with operation of scientific instruments measuring properties of charged particle populations. Impacts can vary from an annoyance to operations at best or lead to mission failure at worst. The threat of spacecraft charging is best mitigated using the traditional approach of designing flight hardware that is not susceptible to damage or operational impacts from large surface potentials and electrostatic discharges. However, this is not always possible and in some applications there is an advantage for operations teams to mitigate charging threats by avoiding critical flight operations during environmental conditions where strong charging might exist. In these cases, flight constraints (or flight rules) can be adopted to avoid mission critical operations during strong charging conditions that represent a threat to the vehicle.

Examples where spacecraft charging flight constraints could be useful are radiation belt transits for vehicles destined for operations in benign charging environments that are not designed to withstand severe charging, rendezvous and docking operations within the Earth's radiation belts and auroral regions, refueling or other satellite maintenance operations that are sensitive to large potentials and arcing from charge accumulation, and extravehicular activities of crew in charging environments.

An example where flight constraints were used to protect a spacecraft is the launch of NASA's James Webb Space Telescope in December 2021 [1,2,3]. Launch commit criteria (LCC) based on solar proton flux were used to avoid single event upsets in flight critical avionics early in the mission. A novel technique applied for this launch included LCC for the geomagnetic Kp index and >2 MeV electron flux levels to avoid the possibility of ESD damage to the spacecraft from surface and internal charging, respectively, during transit of the Earth's outer radiation belt. In this case, the spacecraft was designed to withstand the radiation belt charging environments, but the constraints were implemented as an additional risk mitigation procedure to assure successful deployment and operations of the high value spacecraft.

This paper first introduces the use of space environment flight constraints and provide examples of where they have been used in the past. We next describe the space weather launch commit criteria for solar particle events, internal charging, and surface charging adopted by JWST Program to protect the spacecraft from severe space environments during initial operations in the first 18 hours following launch. Finally, we summarize the space environment conditions during the JWST launch operations and show that space weather turned out to not be a constraint for launch.

II. SPACE ENVIRONMENT LAUNCH CONSTRAINTS

A. Environment Flight Constraints

Environmental constraints on flight operations are operational controls used to protect space systems from exposing hardware or crew to extreme environments that exceed the capabilities of the system design. Good system design for flight hardware to operate during and after exposure to the most extreme environments expected during a mission is the preferred choice to mitigate environmental threats. However, in some cases this cannot be done or an environmental threat shows up after a system design is complete and cost and schedule pressure requires the operational approach. While operational space environmental controls don't require modification of flight hardware, they do require a capability for monitoring the environment in near real time and an ability to change operations at the last minute based on whether the environment exceeds the flight constraint. Operational controls are best used for short periods of time when environments exceed the capability of the design.

Flight constraints used for spacecraft launch operations in the past and present have mostly been related to terrestrial environments and include weather conditions at launch site that impact launch operations including wind, temperature, cloud cover, precipitation, and lightning. Downrange weather conditions that impact hardware recovery and contingency operations may also be used to constraint launch operations if crew or flight hardware recovery is a program requirement. Illumination requirements (day/night) may also be a constraint for system with requirements for optical monitoring systems deployed during the flight operations. In these cases, the LCC associated with the relevant environment is intended to protect the launch vehicle and not the spacecraft.

Space weather flight constraints are operational controls on flight operations used to mitigate the detrimental effects of space environment interactions with flight hardware and crew Examples of space environment threats that can be mitigated to some extent by flight constraints include single event effects in critical avionics and crew dose due to solar particle events, hypervelocity impact damage from meteor showers, ESD due to spacecraft charging in low Earth polar orbits or during transit of the outer radiation belt, and satellite draft due to increased neutral atmospheric density during geomagnetic storms.

Space environment flight constraints are indicated as operational controls for rate driven effects that depend on short term increases in charged particle flux, meteor flux, or thermosphere density and protection of critical flight operations that take place over restricted periods of time that can be deferred until the space environment threat has ended. Flight constraints are not useful for fluence driven effects over long periods of time including such effects as the cumulative total ionizing dose and displacement damage in electronics over a mission, hypervelocity impact damage from sporadic meteors, and satellite drag over the lifetime of a mission.

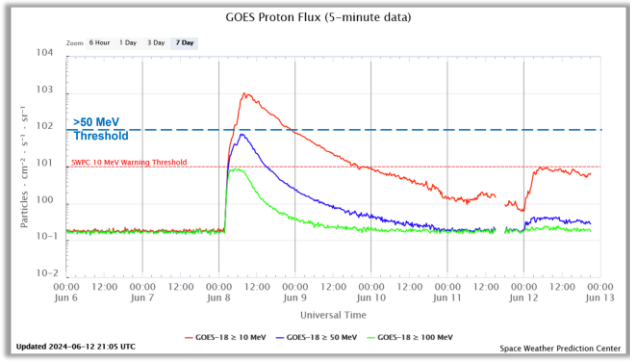


Fig. 1. SPE with Example >50 MeV Proton Constraint. This example is the 8 June 2024 solar particle event with significant flux in the >50 MeV and >100 MeV channels. Even though the SPE exceeded the >10 pfu threshold (red dotted line) for NOAA SWPC to issue an SPE alert, if a flight constraint was based on a >100 pfu threshold (blue dashed line) for >50 MeV protons, then no proton constraint violation would have occurred.

B. Example of Solar Particle Event (SPE) Constraint

Space radiation impacts on launch vehicle avionics and spacecraft operations have been considered for many years where avionics not designed to mitigate single event effects are protected from solar protons and heavy ions through the use of a launch constraint [4,5,6]. Launch providers may use a solar proton constraint even if their avionics are design to mitigate radiation effects for an extra level of precaution during launch operations. Solar proton constraints may also be used to protect satellites during flight critical satellite operations such as proximity operations, rendezvous and docking maneuvers, and flight critical thruster firings. Human spaceflight has a long history of using solar proton constraints and radiation monitoring to protect flight crews from increased radiation dose during extravehicular activities and for providing alerts when crews need to move to more protected areas in spacecraft during increased radiation events.

Solar proton constraints typically take the form of critical operations are "no go" when

$$J(>N\ \text{MeV}) > M\ \text{protons/cm}^2\text{-sec-sr} \qquad (1)$$

where J(>N MeV) is the measured integral proton flux above an energy threshold N and M is integral proton flux constraint level. The critical flight operation may be the decision for a launch, a thruster firing which modifies a flight trajectory, or some other critical launch vehicle or spacecraft operation.

Figure 1 shows an example from the SPE with an onset early on 8 June 2024. NOAA's Space Weather Prediction Center (SWPC) issued an alert for a >10 MeV proton event soon after onset when the >10 MeV proton flux exceeded the threshold level of 10 pfu (where pfu = *particle flux unit* with units of particles/cm^2-sec-sr). The SPE exceed the NOAA SWPC 10

pfu threshold (red dotted line) for almost two days. However, if a solar proton flight constraint was adopted to protect an important avionics system susceptible to single event upsets using the 100 pfu level for >50 MeV protons (blue dashed line), then there would not have been a solar proton constraint violation for this SPE because the peak >50 MeV proton flux was only 78.6 pfu, less than the constraint value.

C. Launch Operations Delayed Due to Space Environments

Launch constraints find wide use in launch operations, and many launches have been delayed due to terrestrial weather conditions including wind, clouds, rain, and lightning. While space environments have been a concern for launches for many years, there have been only five occasions for which launch operations have been delayed due to space environments.

- **Space Shuttle STS-51 (NASA) [7]**
  Payloads: ACTS satellite, OERFEUS-SPAS satellite
  Cause: Perseid meteor shower (peak on 11 August 1993)
  Scheduled launch: August 1993
  Delay: 4 August launch postponed to 12 August to avoid Perseid meteor shower peak on 11 August

- **Athena I Launch Vehicle (NASA/DoD) [8]**
  Payload: Kodiak Star spacecraft
  Cause: Solar particle event (onset 24 Sep 2001)
  Scheduled launch: 24 September 2001\
  Delay: 6 days to 30 September

- **Antares Launch Vehicle (NASA) [9]**
  Payload: Cygnus resupply vehicle to ISS
  Cause: Solar particle event (onset 7 Jan 2014)
  Scheduled launch: 8 January 2014
  Delay: 1 day to 9 January

- **Delta IV Launch Vehicle (DoD) [10]**
  Payload: GPS IIF-5 satellite
  Cause: Solar particle event (onset 20 Feb 2014)
  Scheduled launch: 21 February 2014
  Delay: 19 minutes (to end of launch window)

- **Falcon 9 Launch Vehicle (SpaceX) [11]**
  Payloads: 21 Starlink Group 6-1 satellites
  Cause: Solar particle event and geomagnetic storm (onset 26 Feb 2023)
  Scheduled launch: 27 February 2023
  Delay: 4+ hours

III. JWST LAUNCH CONSTRAINTS

An example where flight constraints were used to protect a spacecraft instead of the launch vehicle is the launch of NASA's James Webb Space Telescope in December 2021 where space weather launch constraints based on >50 MeV and >100 MeV solar proton flux were used to protect the vehicle from single event effects and the geomagnetic Kp index and >2 MeV electron flux were used to avoid ESD damage to the spacecraft from surface and internal charging, respectively, during transit of the Earth's outer radiation belt. A summary of the space weather launch constraints and the NOAA SWPC data sources used to monitor the constraints in real-time is given in Table 1. In this case, the JWST spacecraft was designed to withstand the radiation belt charging environments, but the space weather constraints were implemented as an additional risk mitigation procedure to assure successful deployment and operations of the high value spacecraft [1,2,3]

The three space environment launch constraints were used during the JWST launch operations to avoid the chance of severe space weather events including a) a solar proton flux constraint to avoid high single event upset rates in mission critical avionics due to a solar particle event during the first 18-hours of flight, b) an energetic electron constraint to avoid ESD during transit of the outer radiation belt, and c) a Kp constraint to avoid ESD due to surface charging during the radiation belt transit.

The JWST Program had initially planned to use a solar proton launch constraint to protect sensitive avionics during initial flight operations. However, the JWST Program did not initially have any plans to include launch constraints for spacecraft charging. A team of charging experts was assembled by the NASA Engineering and Safety Center (NESC) to conduct an independent study of the solar proton constraint and consider if there was an advantage in using additional constraints to protect the spacecraft from ESD during the radiation belt transit. Details of this independent analysis of the proton and spacecraft charging constraints as well as the development of the spacecraft charging LCC are described in detail in Minow et al., 2018 [1] with the development of the charging constraints summarized in the follow two sections. Discussion on development and evaluation of the solar proton launch constraint is out of scope for this paper.

A. Internal Charging Constraint

Evaluations of internal charging risks considered the possibility that extreme electron environments in the outer radiation belt could exceed the flux levels at which arcing was observed in laboratory tests of cables and avionics boxes used in the JWST spacecraft design. If the extreme environments were insufficient to result in charging to levels where arcing would occur then there was no reason to implement a launch constraint. Only in the case where observed electron flux would exceed the levels at which tests showed arcing would it be helpful to use a launch constraint.

The areas of JWST most vulnerable to internal charging during transit of the radiation belts are dielectric materials protected only by very thin electron shielding. Of initial concern were unshielded (i.e., no braid or foil EMI shield) cables under blankets, since the discharge of cable insulators could pose a risk to sensitive electronics interfaces. Unshielded cable sections attached to sensitive telemetry interfaces on the Optical Telescope Element (OTE) were analyzed for ESD risk

Table 1. JWST Space Weather Launch Commit Criteria and Data Sources

Constraint	NOAA SWPC Data Source
Protons (Threat: single event upsets from SPE protons, heavy ions)	
From L-12 hours to L-10 minutes, NO-GO if	
There is an active space weather advisory warning or extended warning issued by NOAA SWPC for a proton event of >100 MeV integral flux >1 pfu expected, or,	**NOAA SWPC e-mail subscription products:** https://www.swpc.noaa.gov/content/subscription-services WARNING: Proton 100 MeV Integral Flux >1 pfu expected
Any time the >50 MeV integral proton flux > 5 pfu	**NOAA SWPC GOES real-time proton flux:** https://www.swpc.noaa.gov/products/goes-proton-flux
>2 MeV Electrons (Threat: electrostatic discharge from internal charging)	
From L-5 hours to L-10 minutes, NO-GO if	
>2 MeV integral electron flux >4.98x10^4 pfu measured at GOES West (GOES 17)	**NOAA SWPC GOES real-time electron flux:** https://www.swpc.noaa.gov/products/goes-electron-flux
Geomagnetic storm electrons (Threat: electrostatic discharge from surface charging)	
From L-1 hours to L-10 minutes, NO-GO if	
Kp ≥ 4	**NOAA SWPC GOES real-time planetary k index:** https://services.swpc.noaa.gov/json/planetary_k_index_1m.json

and found to have a small positive margin against the largest expected ESD events on those cable sections based on electron beam cable test data from Northrop Grumman and ESD immunity testing of the relevant integrated circuits at GSFC [12].

Further electron beam testing at NASA's Goddard Space Flight Center on shorter cable sections verified a small positive margin. Given the typical large uncertainties associated with spacecraft charging analysis and the stochastic nature of ESD events, there was some residual concern with the small margin against damaging ESD for the OTE cables based solely on arc magnitude versus electronics susceptibility. When the data are examined from the perspective of expected electron fluence before the first large arcs are expected to occur, more margin is found.

In comparing the statistics of electron flux in three electron channels from the GOES spacecraft over a period of years, it was found that there were no cable internal charging limit violations for 75 keV and 275 keV electrons using GOES observations. However, violations of the >2 MeV constraint were possible for avionics boxes. Therefore, monitoring the 4 hours prior to launch is recommended to best characterize the internal charging electron environment at the time of launch and using 50% of the hardware limits for internal charging launch constraints is recommended to best balance hardware risk versus launch accessibility. The study found no requirement for a launch constraint for the cables. Electron particle fluence limits at time of launch will need to be compared with GOES real-time observations and, therefore, must be appropriately scaled for geostationary orbits.

An electron transport analysis was performed on the most at-risk unshielded cables that are separated from space by only a single-layer Kapton® XC blanket or a multilayer blanket, and on an electronics box with the smallest amount of electron shielding, to determine an acceptable environmental electron fluence while in the radiation belts. Cable and interface testing demonstrated a small positive margin for worst-case cable discharges versus the corresponding interface circuits. Post-test analysis demonstrated that large arcs that approach the damage threshold for at-risk cables occur only after absorbing approximately 450 nC/cm^2 (areal charge density) of charge, equivalent to 2.81e12 electrons/cm^2. This value was taken as the absorbed fluence limit for the cables. Smaller arcs that could possibly cause upsets can occur at much lower absorbed fluence but are not considered a mission risk because the affected circuits are powered down during the radiation belt transit.

Electron threshold limits for the internal charging constraint were established by comparing statistical estimates of extreme electron flux at energies relevant to internal charging with laboratory measurements used to determine the flux limits where arcing of the susceptible hardware would start to take place. Figure 2. shows the calculated flux limits for the cable and box test for the 95%, 99%, and 100% electron flux at geosynchronous orbit. Columns 1 and 2 correspond to the cable 75- and 275-keV differential flux limits, while column 3 is the >2-MeV integral flux box limit. This figure shows that, for all thresholds used in this assessment, the JWST AE9 environments calculated are all lower than the allowable fluence thresholds. This means that, regardless of the environment limit considered, the actual hardware limit is not exceeded in 999 3-hour Monte Carlo runs. An AE9 model limit prevents more than 999 Monte Carlo runs, so the total time represented by these runs is 2,997 hours. To increase the likelihood of capturing extreme events, the AE9 model was run for 3 years for geostationary orbit at the GOES West longitude, and 999 Monte Carlo runs were perfomed with the results scaled as described. The extreme values in the results of those runs agree well with extreme values from the GOES West data and exceed the allowable limits for the electronics box, although infrequently (~0.01% of the time).

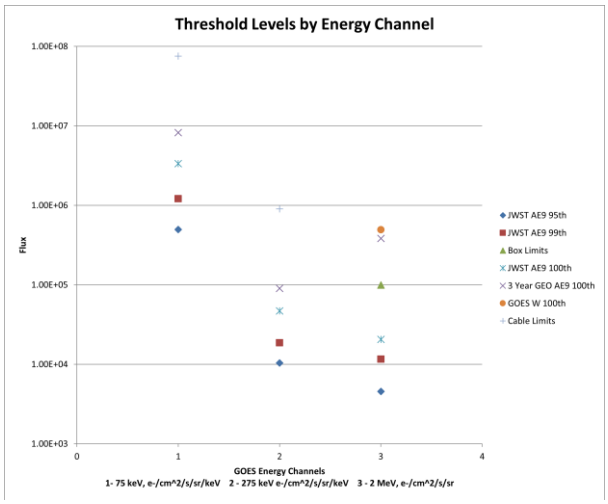


Fig. 2. Cable and Box Threshold Flux Limits. Columns 1, 2 and 3 are the 75 keV and 275 keV differential flux and >2 MeV integral flux, respectively. Comparison of estimated extreme electron environments with measured limits for hardware, details are provided in the text.

These results demonstrate a value in using a >2 MeV electron flux constraint to avoid the chance of an electron environment in the outer belt exceeding the limit where arcing begins to occur during the radiation belt transit. The box limit before arcing was approximately $1x10^5$ electrons/cm^2-sec-sr for >2 MeV electrons, so a threshold of $1x10^5$ electrons/cm^2-sec-sr was chose for the constraint, a value of half the box limit.

B. Surface Charging Constraint

A NASA and Air Force Charging Analyzer Program (Nascap)-2k surface charging analysis of the JWST spacecraft completed in 2008 showed significant surface charging levels from -7 kV to -12 kV while in a modeled geosynchronous substorm environment [13]. However, the same model showed the magnitude of surface potentials were less than 10 V for quiescent plasma environments in geosynchronous orbit. Based on these results, the one of the findings reported in the 2008 study [13] was the JWST Program would benefit from the reduced risk for ESD due to large negative surface potentials if a monitoring system was used to avoid extreme charging environments in the outer radiation belt during the time required for the spacecraft to transit the belts.

The Nascap-2k analysis performed in 2008 used material properties and a spacecraft configuration with JWST in the fully deployed stage during the radiation belt transit which was the plan at the time. While some spacecraft materials and the plans for the final flight configuration of the spacecraft during the radiation belt transit changed over the years, there is still the expectation that significant levels of surface charging could occur in a geosynchronous orbit sub-storm environment. It has been known for many years that substorm environments (e.g., storm periods with $K_p \geq 6$) in the geosynchronous orbit can charge spacecraft to considerably large negative potentials, consistent with the values obtained in the 2008 model [14, 15, 16, 17].

GOES is the only satellite available to US programs that can be used for real-time monitoring of outer belt electron environments. The GOES charged particle instruments are appropriate for solar energetic particle and internal charging observations so initially the GOEs data was evaluated for use in developing an surface charging constraint.

The lowest energy channels for the MAGED instrument on GOES (i.e., the 75-keV and 125-keV differential particle flux measurements) were explored for feasibility. Since these are the lowest energies available using the GOES real-time data stream, it was hoped that a correlation or extrapolation down to the energy channels associated with surface charging (a few tens of eV) would be appropriate for a launch constraint. Unfortunately, after sufficient analysis, this was found not to be a viable option for surface charging commit criteria. Additionally, the plasma environment associated with surface charging is a localized phenomenon and not easily extrapolated to other regions in the plasmasphere [18].

The GOES-16 and GOES-17 satellites, launched November 2016 and March 2018, respectively, are both equipped with a Magnetospheric Particle Sensor Low (MPS-LO) low energy charged particle instrument that is a component of the Space Environment In Situ Suite (SEISS) instrument package. MPS-LO can detect protons and electrons in the 30 eV to 30 keV energy range, which is appropriate for monitoring surface charging environments in GEO. This instrument offers the possibility for monitoring surface charging risks in real time after the instruments are declared operational by NOAA by using the data to estimate the >10 keV integral electron flux or the average electron temperature <Te> that have been shown to be effective metrics for charging in geostationary orbit [19,20] However, at the time the NESC 2018 report [1] was written, the MPS-LO instrument was still undergoing initial checkout activities, which had to be completed before the data can be declared operational and was not available for supporting flight operations. Indeed, as of today this data is still not available from NOAA SWPC as an operational product.

Since direct real-time measurements of electron environments in geostationary orbit were not available, an alternative approach had to be used. A second constraint method was studied using a geomagnetic index as LCC (i.e., K_p value), which is a mid-latitude geomagnetic storm index. NASA's Van Allen Probes routinely traversed the radiation belts from August 2012 through the end of the mission in summer of 2019. Neergaard Parker and Minow [ref. 21] analyzed Van Allen Probe surface charging data from time of launch in 2012 through 2014 and looked for any correlation between surface charging events and K_p value. Figure 3. shows the number of charging events normalized by the total number of orbits versus the K_p value at time of apogee for Van Allen Probe-A (blue), Van Allen Probe-B (red), and both spacecraft (black). The K_p = 4 value had the largest number of charging events, seeing

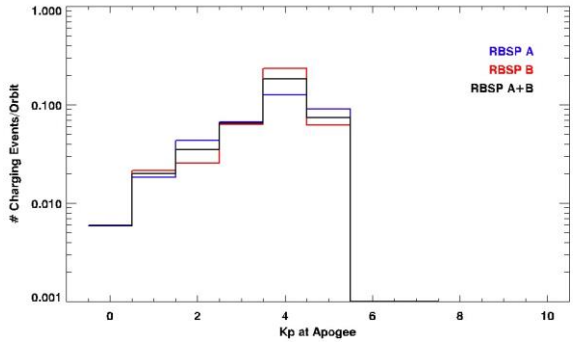


Fig.3. Van Allen Probes Charging Events as function of Kp for 2012 to 2014. The number of charging events for each Kp level (at apogee) is normalized by the number of orbits.

surface charging ~20% of the time when K_p was equal to 4. The study showed that the satellites experienced surface charging 2.5% of the total time (orbits). This shows an expected increase in surface charging events for increasing K_p value up to K_p = 4, after which the number of charging events begins to decrease. A note of caution with this plot: during the 3 years of data for this assessment, there were approximately 30 events for $K_p \geq 5$; therefore, the statistics in those bins are not complete. Charging levels would be expected to continue to climb for increased K_p values. However, O'Brien found a similar rollover effect in surface charging events on the Intelsat satellite (see Figure 1 in [22]). We note that more recently that Bodeau [23] and Ganushkina et al. [24] have argued that Kp is not a good parameter for predicting surface charging in GEO due to the poor correlation in the 3-hour Kp index with measured surface potentials on GEO spacecraft. Likely their poor results are due to the use of 3-hour Kp indices while we chose to use the real-time Kp index provided by NOAA SWPC at 1-minute time resolution for monitoring the JWST launch constraint.

While the value of Kp proxy to be chosen for the surface charging constraint was a risk management decision for the JWST Program, choice of a Kp constraint value that is too common would result in low launch availability. *Kp* data from 1980 to 2014 was used to check the number of occurrences for the various index values. Figure 4. shows the percentage of time that the K_p index was a certain value across all data (black), for the period of solar maximum (red), and for the period of solar minimum (blue). The percentage of time is defined as the number of hours in the database that the Kp level was at a given value, divided by the total number of hours in the database, multiplied by 100. Note that for the periods of all data and solar maximum, the Kp level begins to fall off above Kp = 3, with Kp levels greater than 5 occurring less than 5% of the time. The inset box in Figure 4. shows launch availability for Kp = 4, 5, and 6 for the three periods described. Note that with increasing Kp value, the launch availability increases because the number of occurrences decreases. For the period of solar minimum, the launch availability is greater. As JWST was launched just after the solar minimum period between Solar Cycle 24 and Solar Cycle 24, it is expected that the geomagnetic storm frequency

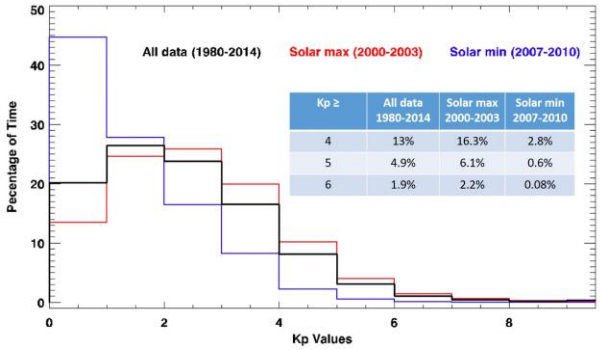


Fig. 4. Launch Availability as a Function of Kp. Kp statistics for all data over a period from 1980 to 2014 (black), 2000 – 2003 solar maximum (red), and 2007 – 2010 (solar minimum) provide estimates of how often a launch would be deferred due the choice of the Kp constraint level.

would be less than the numbers reported for all the data and for the period of solar maximum alone.

The JWST Program adopted the value Kp ≥ 4 for the surface charging constraint, balancing the benefits of a conservative lower Kp value to avoid charging against the reduced launch availability. Based on Figure 4., the probability of having a Kp value greater than or equal to Kp=4 was 2.8 giving a launch availability better than 97% for the near solar minimum period of the JWST launch.

In addition to the risk reduction offered by the Kp constraint, the risk of surface charging along the JWST flight trajectory was relatively low. Surface charging in the outer radiation belt is known to be most common in the midnight to dawn sector and the range of JWST flight trajectories depending on launch date all passed from the noon sector through the pre-midnight sector while in the radiation belts so the flight trajectory was located in regions with lower probability of surface charging events [1,2].

IV. JWST LAUNCH OPERATIONS

JWST launch was initially scheduled for 16 December 2021, but was delayed multiple times due to issues unrelated to space weather. The space weather team started monitoring the state of the space environment at this time for situational awareness and to start preparing to operations once the final launch date was set. The final launch window opened at 12:20 UTC on 25 December 2021 and the real-time space weather support for launch operations started at 12 hours before launch (L-12 hours) on 24 December. Space environment data was continuously monitored for constraint violations and reported to the JWST launch team using the schedule in Table 2.

Space environment did not turn out to be a constraint for JWST launch. While the >2 MeV electron flux in geostationary orbit exceeded the $1x10^3$ electrons/cm^2-sec-sr level where NOAA SWPC issues a radiation belt alert during the launch operations, the

Table 2. JWST LCC Monitoring Schedule

Monitoring and Report	Event
L-12 hrs to L-10 min	Solar proton monitoring
L-6 hrs	Solar proton report for Ariane 5 fueling poll
L-5 hrs to L-10 min	>2 MeV electrons
L-1 hr to L-10 min	Kp
L-10 min	All-inclusive Go/No-Go for launch

peak electron flux was always less than the 4.98×10^4 electrons/cm^2-sec-sr constraint level by about an order of magnitude. Internal charging by energetic electrons was never a threat to the spacecraft. Kp levels values of Kp=3 and Kp=4 were present on 20 and 21 December due to some minor geomagnetic storm activity, but by the time launch operations started on 24 December the Kp levels had dropped to values of Kp = 1 and 2. There was one period of Kp=3 during the launch operations but otherwise Kp remain at 2 or less ad the Kp≥4 constraint was never violated. Finally, we note that the >50 MeV and >100 MeV protons were at background levels during the entire period of launch operations and never represented a risk of violating the solar proton constraints.

JWST was successfully launched at 12:20 UT on 25 December at the opening of the launch window. Space weather had no impact on the initial flight operations including the deployment of the major satellite structural elements. Transit from Earth to the halo orbit about the Sun-Earth L2 point was successful and JWST has been conducting science operations since July 2022..

ACKNOWLEDGMENT

Real-time data and space weather products from the GOES satellites and international magnetometer stations contributing to the Kp index were provided by NOAA's Space Weather Prediction Center. The authors received NASA support from NESC TI-15-01079.

REFERENCES

[1] Minow, J.I., L.N. Parker, Y. Zheng, R.M. Meloy, J. Buhler, R.R. Graber, and R.L. Ladbury, James Webb Space Telescope (JWST) Space Environment Launch Constraints, NESC-RP-15-01079, 1 November 2018.

[2] Minow, J.I., R. Meloy, LN. Parker, and Y. Collado-Vega, Space Weather Launch Constraints for JWST, Applied Space Environments Conference 2023, Huntsville, AL, 9 – 13 October 2023.

[3] Minow, J., Space Weather Support for the James Webb Space Telescope Launch, NOAA Space Weather Workshop, 15 – 19 April 2024, Boulder, CO. (invited)

[4] Mazur, J. E., *et al*., ATR-2008 (8073)-3, The Aerospace Corporation, October 2008.

[5] Minow, J.I., and L.N. Parker, Evaluating Solar Proton Constraints on Flight Operations, *European Space Weather Week*, Leuven, Belgium, 5 – 9 November 2018.

[6] DeStefano, A.M., M.L. Goodman, and R.M. Suggs, The Probability of False Go/No-Go Determined by GOES Proton Flux: Proposed Launch Constraints for Avoiding Damaging Solar Energetic Particle Events, NOAA Space Weather Workshop, Westminster, CO, 16 – 20 April 2018.

[7] Legler, R.D., and F.V. Bennett, Space Shuttle Missions Summary, NASA/TM-2011-216142, Mission Operations, Johnson Space Center, September 2011.

[8] Sardonia, J.E., and J.T. Madura, Kodiak Star: An Overview of Operational Weather Support at the Kodiak Launch Complex for Alaska's first Orbital Space Launch, Paper 39061, 10th Conference on Aviation, Range, and Aerospace Meteorology, American Meteorological Society, Portland, Oregon, 13 – 16 May 2002

[9] Graham, W., ORB-1: Antares Successfully Launches Cygnus En Route to ISS, NASA Space Flight, 9 January 2014, URL:https://www.nasaspaceflight.com/2014/01/orbitals-antares-loft-cygnus-orb-1-mission/

[10] Evans, B., Workhorse Delta IV Returns to Flight with Rousing Nighttime Launch of GPS IIF-5 Satellite, AmericaSpace, 2014. URL:https://www.americaspace.com/2014/02/21/workhorse-delta-iv-returns-to-flight-with-rousing-nighttime-launch-of-gps-iif-5-satellite/

[11] Pultarova, T., Powerful Solar Storm Delays SpaceX Rocket Launch, Stalls Oil Rigs in Canada Amid Aurora-palloza, Space.com, 28 February 2023. URL:https://www.space.com/solar-storm-delays-spacex-launch-supercharges-auroras

[12] Bodeau, M., Impact of ESD from Unshielded Twisted Pair Insulation on Key JWST OTE Circuits, Northrop Grumman IOC, 16-JWST-0116 2016.ST58MB.013, May 26, 2016.

[13] Neergaard Parker, L. and Minow, J. I., Spacecraft Surface Charging Analysis for JWST, ESTSG-FY08-00348, February 2008.

[14] DeForest, S. E. (1972), Spacecraft charging at synchronous orbit, *J. Geophys. Res.*, 77(4), 651–659, doi:10.1029/JA077i004p00651.

[15] Garrett, H.B., The Charging of Spacecraft Surfaces, Rev. of Geophys. And Space Phys., Vol. 19, No. 4, pp. 577-616, 1981.

[16] Olsen, R.C., Record Charging Events from Applied Technology Satellite 6, J. Spacecraft and Rockets, Vol., 24, No. 4, pp. 362-366, 1986.

[17] Thomsen, M. F., M. G. Henderson, and V. K. Jordanova (2013), Statistical properties of the surface-charging environment at geosynchronous orbit, *Space Weather*, 11, 237–244, doi:10.1002/swe.20049.

[18] Koons, H., J. Mazur, A. Lopatin, D. Pitchford, A. Bogorad, R. Herschitz, Spatial and Temporal Correlation of Spacecraft Surface Charging in Geosynchronous Orbit, *Journal of Spacecraft and Rockets*, Vol. 43, No. 1, 2006.

[19] Thomsen, M. F., M. G. Henderson, and V. K. Jordanova (2013), Statistical properties of the surface-charging environment at geosynchronous orbit, *Space Weather*, 11, 237–244, doi:10.1002/swe.20049.

[20] Zheng, Y., Ganushkina, N. Y., Jiggens, P., Jun, I., Meier, M., Minow, J. I., et al. (2019). Space radiation and plasma effects on satellites and aviation: Quantities and metrics for tracking performance of space weather environment models. *Space Weather*, 17, 1384–1403. https://doi.org/10.1029/2018SW002042

[21] Parker, L.N., and J.I. Minow, Spacecraft charging in geostationary transfer orbit, Abstract SM24A-05, presented at 2014 Fall Meeting, AGU, San Francisco, CA, 15-19 Dec, 2014.

[22] O'Brien, T. P., SEAES-GEO: A Spacecraft Environmental Anomalies Expert System for Geosynchronous Orbit, *Space Weather*, Vol. 7, 2009.

[23] Bodeau, M. (2015). Review of better space weather proxies for spacecraft surface charging. IEEE Transactions on Plasma Science, 43(9), 3075–3085. https://doi.org/10.1109/TPS.2015.2441038

[24] Ganushkina, N. Y., Swiger, B., Dubyagin, S., Matéo-Vélez, J.-C., Liemohn, M. W., Sicard, A., & Payan, D. (2021). Worst-case severe environments for surface charging observed at LANL satellites as dependent on solar wind and geomagnetic conditions. Space Weather, 19, e2021SW002732. https://doi.org/10.1029/2021SW002732